THE JOURNAL OF PHYSICAL CHEMISTRY A
Article
pubs.acs.org/JPCA

Theoretical Rationalization of the Emission Properties of Prototypical Cu(I)−Phenanthroline Complexes

G. Capano,[†,‡] U. Rothlisberger,[‡] I. Tavernelli,[‡] and T. J. Penfold*[,§]

[†]École Polytechnique Fédérale de Lausanne (EPFL), Laboratoire de spectroscopie ultrarapide, ISIC, FSB Station 6, CH-1015 Lausanne, Switzerland

[‡]École Polytechnique Fédérale de Lausanne (EPFL), Laboratoire de chimie et biochimie computationnelles, ISIC, FSB-BCH, CH-1015 Lausanne, Switzerland

[§]SwissFEL, Paul Scherrer Institute, CH-5232 Villigen, Switzerland

Supporting Information

ABSTRACT: The excited state properties of transition metal complexes have become a central focus of research owing to a wide range of possible applications that seek to exploit their luminescence properties. Herein, we use density functional theory (DFT), time-dependent DFT (TDDFT), classical and quantum mechanics/molecular mechanics (QM/MM) molecular dynamics (MD) simulations to provide a full understanding on the role of the geometric and electronic structure, spin−orbit coupling, singlet−triplet gap and the solvent environment on the emission properties of nine prototypical copper(I)−phenanthroline complexes. Our calculations reveal clear trends in the electronic properties that are strongly correlated to the luminescence properties, allowing us to rationalize the role of specific structural modifications. The MD simulations show, in agreement with recent experimental observations, that the lifetime shortening of the excited triplet state in donor solvents (acetonitrile) is not due to the formation of an exciplex. Instead, the solute−solvent interaction is transient and arises from solvent structures that are similar to the ones already present in the ground state. These results based on a subset of the prototypical mononuclear Cu(I) complexes shed general insight into these complexes that may be exploited for development of mononuclear Cu(I) complexes for applications as, for example, emitters in third generation OLEDs.

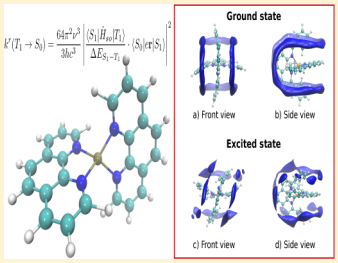

INTRODUCTION

Owing to their luminescence properties and versatility, transition metal complexes have been subjected to an extensive research effort aimed at a wide range of possible applications. The archetypal luminescent transition metal complex is tris(bipyridyl)ruthenium(II), $[Ru(bpy)_3]^{2+}$.[1−3] Here, the amalgamation of a relatively easily oxidized d^6 metal ion and the electron accepting bipyridine ligands gives rise to low-lying excited states exhibiting metal-to-ligand charge transfer (MLCT) character. Once populated, by either photoexcitation or electrical excitation, the participation of the metal ion in these excited states not only enables large spin−orbit coupling (SOC) and permits ultrafast intersystem crossing (ISC)[4,5] but also promotes a strong $T_1 \rightarrow S_0$ radiative transition that has a lifetime of ∼10 μs.[6]

The understanding of the photophysics of $[Ru(bpy)_3]^{2+}$ has logically been extended to a large class of complexes containing second and third row transition metal, such as Re(I),[7−11] Os(II),[12−15] Pt(II),[16,17] and Ir(III),[18−20] which have found potential applications in organic light-emitting diodes (OLEDs)[21−23] and light-emitting electrochemical cells (LEECs),[24,25] as chemo- and biosensors,[26,27] or as fluorophors in cell imaging.[28]

It is widely acknowledged that complexes containing second and third row transition metal ions presently form the most stable and versatile emitters. However, these metals are unappealing for commercial applications due to their high cost and low abundance. Similar complexes based upon first row transition metal ions, such as $[Fe(bpy)_3]^{2+}$,[29,30] have a smaller d−d crystal field splitting and consequently suffer from the presence of low-lying nonemissive metal centered transitions that quench the excited state emission. Although these problems can be overcome, to a certain extent, using structural modifications of the ligands to destabilize the metal-centered states,[31,32] this places a large restriction on the structural modifications that can be performed to fine-tune their photophysical properties. Consequently, one of the most attractive methods is to simply remove the metal centered states by adopting a complex based upon d^{10} metal ions, such as Cu(I), Ag(I), Au(I), Zn(II), and Cd(II).[33] Among the most popular are those containing Cu(I) ions,[34] especially those complexed with phenanthrolines ligands (see ref 35 and references therein) that are the focus of the present work.

To understand the photophysical properties of the Cu(I)−phenanthroline complexes, a number of groups have investigated the dynamics on the ultrafast (femtosecond) time scale.[36−43] The general picture that emerges from these studies indicates that following photoexcitation, the complex relaxes

Received: April 22, 2015
Revised: June 11, 2015
Published: June 11, 2015

DOI: 10.1021/acs.jpca.5b03842
J. Phys. Chem. A 2015, 119, 7026−7037

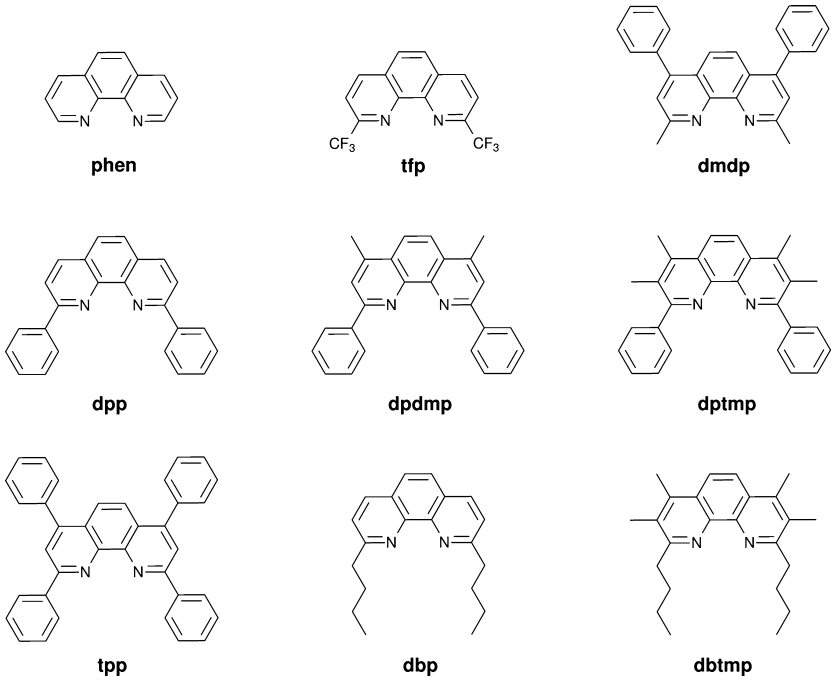

Figure 1. Schematic representation of the nine ligands studied herein and their abbreviated names.

into the lowest singlet excited state in ∼100 fs. This is followed by the structural distortion, associated with the pseudo Jahn−Teller (PJT) instability of the Cu(II) ion, and intersystem crossing (ISC) to the lowest triplet state T_1.[40] This latter process occurs upon two distinct time scales, subpicosecond near the Franck−Condon (FC) geometry and tens of picoseconds, at the flattened (i.e., PJT) geometry.[42,43] Importantly, in the context of their emission properties, these initial steps are completed within a few tens of picoseconds and are broadly equivalent for all of the complexes. Consequently, one would expect that these dynamics should not have a significant impact on the potential application of these complexes.

The same cannot be said for the longer time (picoseconds to microseconds) dynamics associated with the emission from the low-lying excited states. Indeed, following their pioneering work McMillin and co-workers demonstrated that the emission lifetime of these complexes (Table S1, Supporting Information) is strongly dependent upon both structural modifications to the phenanthroline ligands and the environment within which the complex is embedded, especially in the case of solutions.[34,44−47] For the latter they found that emission lifetimes can be significantly shortened in donating solvents (i.e., those behaving as Lewis bases), such as acetonitrile (MeCN),[48] compared to the case for nondonating solvents, such as dichloromethane (DCM). They attributed this quenching to complexation of a solvent molecule (exciplex) that most likely occurs at the metal center, during which the interaction between the Cu(II) atom and the electron-rich donor molecule is thought to stabilize the excited state relative to the ground state, reducing the energy gap and therefore increasing the rate of nonradiative decay.[49] However, a recent time-resolved X-ray absorption spectroscopy study[50] has demonstrated that the transient XAS spectrum is the same for $[Cu(dmp)_2]^+$ (dmp = 2,9-dimethyl-1,10-phenanthroline) in MeCN and DCM. Given the sensitivity of XAS to the coordination number and the structure around the absorbing atom,[51,52] this makes complexation of a solvent molecule very unlikely and therefore the exact nature of the solute−solvent interaction remains undetermined.

Besides the role of the environment, McMillin and co-workers also demonstrated the effect of temperature on the radiative properties of these complexes.[53] Indeed, owing to a relatively small energy gap between the emitting singlet and triplet states, thermal motion is able to promote reverse intersystem crossing (rISC) from the T_1 to S_1 increasing the contribution of the S_1 state to the total radiative decay. Here, the contribution of each state to the emission spectrum is governed by a Boltzmann distribution according to

$$\frac{\mathrm{Int}(S_1\rightarrow S_0)}{\mathrm{Int}(T_1\rightarrow S_0)} = \frac{k^r(S_1\rightarrow S_0)}{k^r(T_1\rightarrow S_0)}\cdot\exp\left(-\frac{\Delta E_{S1-T1}}{k_B T}\right) \quad (1)$$

where k_B is the Boltzmann constant and T is absolute temperature. $\mathrm{Int}(S_1\rightarrow S_0)$, $\mathrm{Int}(T_1\rightarrow S_0)$, $k^r(S_1\rightarrow S_0)$, and $k^r(T_1\rightarrow S_0)$ represent the fluorescence and phosphorescence intensities and corresponding radiative rates, respectively. This mechanism, known as thermally activated delayed fluorescence (TADF) has recently gained significant interest for emitters within third generation OLEDs[54−56] as it relaxes the requirement for a significant $T_1 \rightarrow S_0$ radiative transition and therefore the reliance of these devices on heavy metals such as iridium and platinum.[57]

These previous works have demonstrated both the importance and interest for understanding the luminescence properties of Cu(I)−phenanthrolines, especially the role of the geometric and electronic structure and the solvent. Consequently, in this contribution we use DFT and TDDFT and classical and QM/MM MD simulations to provide a thorough description of the factors influencing the emission from nine prototypical Cu(I)−phenanthroline complexes, namely, $[Cu(phen)_2]^+$, $[Cu(tfp)_2]^+$, $[Cu(dmdp)_2]^+$, $[Cu(dpp)_2]^+$, $[Cu(dpdmp)_2]^+$, $[Cu(dptmp)_2]^+$, $[Cu(tpp)_2]^+$, $[Cu(dbp)_2]^+$, and $[Cu(dbtmp)_2]^+$ (Figure 1). Our quantum chemistry calculations reproduce the trends observed experimentally, providing

DOI: 10.1021/acs.jpca.5b03842
J. Phys. Chem. A 2015, 119, 7026−7037

Table 1. Room Temperature Emission Data for the Nine Cu(I)−Phenanthroline Complexes in MeCN or DCM Compared to Values Calculated Using LR-TDDFT(B3LYP) As Implemented within ADF

	in MeCN		in DCM		calculated				
	exp (nm/eV)	τ (ns)	exp (nm/eV)	τ (ns)	T_1 (eV)	S_1 (eV)	f_{S_1}	$\Delta E_{S_1-T_1}$ (eV)	DHA (deg)
$[Cu(phen)_2]^+$ [d]				<20	0.62	1.22	0.057	0.6	39
$[Cu(tfp)_2]^+$ [c]			665/1.86	165	1.34	1.73	0.038	0.39	74
$[Cu(dmdp)_2]^+$ [a]			770/1.61	80	1.04	1.60	0.123	0.56	58
$[Cu(dpp)_2]^+$ [a]	735/1.69	180	710/1.75	280	1.43	1.66	0.036	0.23	53
$[Cu(dpdmp)_2]^+$ [b]			720/1.72	310	1.31	1.65	0.023	0.34	53
$[Cu(dptmp)_2]^+$ [b]	735/1.69	260	715/1.73	480	1.25	1.66	0.044	0.41	61
$[Cu(tpp)_2]^+$ [a]	765/1.62	120	745/1.66	230	1.30	1.61	0.080	0.31	50
$[Cu(dbp)_2]^+$ [b]	730/1.70	35	715/1.73	150	1.36	1.69	0.036	0.33	75
$[Cu(dbtmp)_2]^+$ [b]	690/1.78	440	670/1.85	920	1.38	1.73	0.045	0.35	70

[a]Reference 71. [b]Reference 72. [c]Reference 73. [d]Reference 74. Dha are the dihedral angles between the ligands.

important insight into the contributing electronic and structural variables. Using the molecular dynamics simulations, we find that in solution the excited state of none of these complexes exhibits the formation of an exciplex. Instead, the solvent−solute interaction is transient and arises from solvent configurations similar to the ones already sampled in the ground state dynamics.

COMPUTATIONAL DETAILS

Electronic Structure Calculations. The structure of the ground and lowest triplet states of the nine Cu(I)−phenanthroline complexes were optimized at DFT(BLYP)[58,59] and DFT(B3LYP)[60] level using Gaussian09.[61] The effect of the weak $\pi-\pi$ interactions were accounted for during the optimizations using the Grimme's D2 dispersion correction.[62] Triple-ζ (Cu) and double-ζ (F, N, C, and H) basis sets with polarization functions were used for all of the electronic structure calculations. The main structural parameters are listed in the Supporting Information in Table S2, and the cartesian coordinates are provided in Tables S13−S30 of the Supporting Information.

The excited state energies were computed using linear response time-dependent density functional theory (LR-TDDFT) using the Tamm−Damcoff approximation and the B3LYP exchange and correlation functional as implemented within the Amsterdam Density Functional (ADF)[63−65] code. The SOC matrix elements were computed with the perturbative approach developed by Wang and Ziegler.[66] A TZP basis set was used for all atoms and scalar relativistic effects were accounted for using the zeroth-order relativistic approximation (ZORA).[67,68] The excited state energies computed at the ground state geometry corresponding to the absorption spectrum are given in Table S3 (Supporting Information).

Finally, it is noted that throughout this work we have computed all emission properties from the optimized T_1 geometry. Though direct comparison with the experimental data also requires the emission to the calculated at the relaxed S_1 geometry, previous studies[39,40,42,43] have demonstrated its similarity to the T_1 state. In addition, due to the weak exchange interaction between the S_1 and T_1 states, which leads to the small $\Delta E_{S_1-T_1}$, the energy gap between these states, $\Delta E_{S_1-T_1}$, is expected to be independent of geometry and therefore close to constant for all nuclear configurations.[56]

Molecular Dynamics Simulations. Classical MD simulations were performed using Amber 12.[69] The standard Amber force field was augmented with additional parameters describing the bonds, angles, and dihedrals involving the copper ion (Tables S4−S12, Supporting Information). The bonding parameters and force constants of these additional parameters were obtained using DFT(B3LYP). The charges were calculated with the restricted electrostatic potential (RESP)[70] method fixing the charge of Cu with the one obtained using the Mulliken method. The classical simulations were performed with a time step of 1 fs. After 1 ns of equilibration, the system was propagated for a further 15 ns, from which all properties were calculated.

The classical MD simulations have been supplemented with Car−Parrinello[75] QM/MM[76,77] MD simulations performed using the CPMD software.[78] These were performed for three of the complexes, namely, $[Cu(phen)_2]^+$, $[Cu(dbp)_2]^+$, and $[Cu(dpp)_2]^+$. Starting from an equilibrated configuration from the classical MD trajectory, the systems were thermalizd for 2 ps. Subsequently, the systems were equilibrated for a further picosecond using two Nose−Hoover thermostats[79,80] (one on the quantum region and one for the classical region) with a coupling frequency of 2000 cm^{-1}. Finally, the MD was run for ∼20 ps from which all of the properties were calculated. In all cases a fictitious electron mass of 600 au and a time step of 0.01 fs were used. The quantum part, which incorporated only the Cu(I)−phenanthroline complex was computed with DFT(BLYP) using Troullier−Martins pseudopotentials[81] to describe the core electrons. The plane-wave cutoff for the expansion of the one-particle orbitals was set to 85 Ry. The effect of weak $\pi-\pi$ interactions was included using the dispersion-corrected atom-centered potential (DCACP) method.[82−84] The validity of the classical MD force fields was assessed by comparing average values and standard deviations of bond length, angles, and dihedrals from classical and Car−Parrinello QM/MM MD trajectories in both the ground and the lowest triplet excited states. These are shown in Figures S2−S4 (Supporting Information).

RESULTS

Emission Properties. Table 1 shows the experimental and computed (TDDFT/B3LYP) emission energies for each of the complexes using the structures optimized using DFT(B3LYP) and given in the Supporting Information. For $[Cu(phen)_2]^+$ we find a small energy gap between the ground and excited states that originates from the large structural distortion in the excited state. This explains its very short lifetime (∼2 ps in MeCN)[41] that is dominated by a large contribution of nonradiative

DOI: 10.1021/acs.jpca.5b03842
J. Phys. Chem. A 2015, 119, 7026−7037

decay.[49] For $[Cu(dmdp)_2]^+$ and $[Cu(tfp)_2]^+$ we observe a large emission energy and a longer emission lifetime, as expected due to the smaller structural distortion. Of these two, $[Cu(dmdp)_2]^+$ exhibits the shorter lifetime due to the smaller energy gap ($S_1 \rightarrow S_0$) and larger oscillator strength. The latter is due to the presence of the phenyl substituents in the 4,7 positions (Supporting Information, Figure S1) that extends the π system away from the metal center, increasing the transition dipole length and therefore the oscillator strength of the transition.[85]

The inclusion of larger substituents (phenyl and *n*-butyl) onto the 2,9 positions has a significant effect on the lifetime. Despite the smaller energy gap with the ground state, $[Cu(dpp)_2]^+$ has a lifetime (in DCM) that is almost a factor of 2 longer than that for $[Cu(tfp)_2]^+$ and a factor of 4 larger than that for $[Cu(dmdp)_2]^+$. In this case the phenyl substituents in the 2,9 positions bring the π system of the ligands toward the metal center and decreases the transition dipole length compared to that for $[Cu(dmdp)_2]^+$. This causes a significant decrease in the oscillator strength (Table 1, 0.123−0.036) and therefore a longer emission lifetime. Compared to the case for $[Cu(tfp)_2]^+$, we find a similar oscillator strength; however, $[Cu(dpp)_2]^+$ has a much larger dihedral angle (Table 1), which leads to a smaller SOC coupling (discussed in the following section). As the radiative rate of the triplet state is expressed

$$k^r(T_1 \rightarrow S_0) = \frac{64\pi^2\nu^3}{3hc^3}\left|\frac{\langle S_1|\hat{H}_{SO}|T_1\rangle}{\Delta E_{S_1-T_1}}\cdot\langle S_0|e\mathbf{r}|S_1\rangle\right|^2 \quad (2)$$

the reduction in SOC reduces the mixing of the S_1 and T_1 states, thus extending the lifetime of the triplet state.

The role of the $\Delta E_{S_1-T_1}$ energy gap, highlighted in eqs 1 and 2, on the luminescence lifetime of the complexes is exemplified by comparison among $[Cu(dpp)_2]^+$, $[Cu(dpdmp)_2]^+$, and $[Cu(dptmp)_2]^+$. Indeed, all three have emission bands centered at similar energies (~1.70 eV); however, their lifetimes in DCM vary by almost a factor of 2. This is correlated to an increase in $\Delta E_{S_1-T_1}$, which is determined by the spatial overlap between the singlet and triplet excited state wave functions.[86] For these complexes, the inductive effect of the methyl substituents in the 3,4,7,8 positions on the phenanthroline ligands pushes the electron density toward the copper ions. This increases the interaction between the unpaired electron on the ligands with the one on the metal centered d-orbitals, due to the smaller spatial separation. As a consequence, we observe a decrease of the contribution of the S_1 fluorescence to the overall radiative emission (eq 1). In addition, a reduction of the mixing of the singlet and triplet state (eq 2) reduces $k^r(T_1)$, which therefore contributes to the extension of the lifetime of the excited state. $[Cu(tpp)_2]^+$ does not follow this trend, because the phenyl substituents in the 4,7 position not only reduce interactions between the unpaired electrons but also, by extending the π system away from the metal d-orbital, increase the dipole length and consequently the oscillator strength, giving rise to a shorter lifetime.

Finally, in terms of the emission lifetime perhaps the most intriguing complexes are $[Cu(dbp)_2]^+$ and $[Cu(dbtmp)_2]^+$. These display strongly contrasting lifetimes, in agreement with similar effects recently observed in related complexes.[87] This has previously been rationalized by the steric hindrance of the 3,8 methyl groups that restrict the conformational freedom of the groups in the 2,9-positions of the phenanthroline ligand and thereby increase the effective steric demand of the ligand. Under such conditions, the complex is expected, as observed, to emit at shorter wavelength and due to the energy gap law exhibit a longer excited state lifetime.[72]

Spin−Orbit Coupling. As previously discussed, large SOC not only permits ultrafast intersystem crossing (ISC) but also promotes a strong $T_1 \rightarrow S_0$ radiative transition. Consequently, understanding the SOC at both the ground and triplet (emitting) states geometries and its dependence on the geometric structure plays an important role in determining the lifetime and luminescence mechanism of these complexes. The first study into the SOC of Cu(I)−phenanthrolines was performed by Nozaki and co-workers[88] on $[Cu(dmp)_2]^+$. Using a semiquantitative approach, they reported that the SOC matrix elements were strongly dependent on the dihedral angle between the two ligands, which they used to explain the slow ISC rate observed at the flattened PJT geometry of the lowest ^{3}MLCT state.

Assuming a one-electron one-center approximation, the SOC operator is expressed as

$$\hat{H}_{SO} = \zeta \sum_i^{N_{el}} \hat{l}_i\hat{s}_i \quad (3)$$

where $\hat{l}_i$ is the angular momentum of electron *i* and $\hat{s}_i$ is the spin operator of electron *i*. ζ is the spin−orbit coupling constant, proportional to the atomic number and inversely proportional to the mean cubic radial distribution (r^{-3}) of the electron, and is therefore responsible for the so-called *heavy atom effect*. However, for a full understanding of the SOC mechanism, one must also consider the integral over the two states involved:

$$[\hat{H}_{SO}]_{ij} = \langle \Psi_{S_i}|\hat{H}_{SO}|\Psi_{T_j}\rangle \quad (4)$$

This integral, sometimes referred to as the *internal effect*, depends principally on the character of the states involved, as outlined for organic systems by El-Sayed.[89] In his work, El-Sayed highlighted that to achieve effective SOC, any change in spin must be accompanied by a corresponding change in angular momentum, so that total angular momentum is conserved. Consequently, SOC between the MLCT states of transition metal complexes must work between the dπ* configurations involving d orbitals of different orientations.[90] Indeed, this is why, despite the heavy atom effect, the SOC for Au(I) complexes is generally smaller than the one for analogous Cu(I) complexes, as the larger crystal field splitting leads to a smaller contribution of d-orbitals in the excited state.[91]

Table 2 shows the significant (>10 cm^{-1}) SOC matrix elements for the nine Cu(I)−phenanthroline complexes at both the Franck−Condon and lowest triplet state geometries. At the Franck−Condon geometry, the complexes that exhibit no dihedral distortion show significant SOC matrix elements (>10 cm^{-1}) between the S_1, S_2 states and the triplet manifold. Indeed, $[Cu(dmdp)_2]^+$ exhibits spin−orbit coupling characteristics very similar to those described by Nozaki and co-workers[88] for $[Cu(dmp)_2]^+$. This demonstrates that, in contrast to the oscillator strengths and excited state energies reported in the previous section, the phenyl substituent in the 4,7 positions that contain only light elements, do not have a large impact on the magnitude of the SOC matrix elements. At the equilibrium geometry the main coupling is between the S_1 and T_1 and is 263 cm^{-1}. This arises from the spin−orbit integrals between the main excited state configurations, $\langle d_{yz}\rightarrow\pi_1^*|\hat{H}_{SO}|d_{xz}\rightarrow\pi_1^*\rangle$ and

DOI: 10.1021/acs.jpca.5b03842
J. Phys. Chem. A 2015, 119, 7026−7037

Table 2. Main (>10 cm^{-1}) Spin−Orbit Coupling Matrix Elements (in cm^{-1}) between the Low-Lying States of the Nine Cu(I)−Phenanthroline Complexes at the Ground State (GS) and ^{3}MLCT Flattened Geometries[a]

	GS		^{3}MLCT	
	$[\hat{H}_{SO}]_{ij}$	∠DHA	$[\hat{H}_{SO}]_{ij}$	∠DHA
$[Cu(phen)_2]^+$	86 (1,1)	90	13 (1,1)	39
	266 (1,2)			
	33 (2,3)			
	306 (2,4)			
$[Cu(tfp)_2]^+$	280 (1,1)	90	50 (1,1)	74
	44 (1,2)			
	317 (2,4)			
$[Cu(dmdp)_2]^+$	263 (1,1)	88	25 (1,1)	58
	32 (1,2)		32 (1,2)	
	15 (1,3)			
	26 (2,2)			
	210 (2,3)			
	205 (2,4)			
$[Cu(dpp)_2]^+$	29 (1,1)	54	21 (1,1)	53
$[Cu(dpdmp)_2]^+$	38 (1,1)	54	28 (1,1)	53
	16 (2,4)		20 (1,2)	
			13 (1,3)	
$[Cu(dptmp)_2]^+$	39 (1,1)	65	23 (1,1)	58
	16 (2,4)			
$[Cu(tpp)_2]^+$	26 (1,1)	51	19 (1,1)	50
$[Cu(dbp)_2]^+$	143 (1,1)	86	37 (1,1)	75
	15 (1,2)			
	232 (1,3)			
	182 (2,2)			
	237 (2,4)			
$[Cu(dbtmp)_2]^+$	125 (1,1)	83	34 (1,1)	70
	232 (1,3)			
	40 (1,4)			
	19 (2,1)			
	177 (2,2)			
	25 (2,3)			
	227 (2,4)			

[a]The numbers in brackets (*i*,*j*) represent the singlet and triplet excited states between which the coupling is acting. DHA is the dihedral angle between the ligands in degrees (deg).

$\langle d_{xz}\rightarrow\pi_2^*|\hat{H}_{SO}|d_{yz}\rightarrow\pi_2^*\rangle$, that contribute to the excited state wavefunction. Here d_{yz} is the HOMO, d_{xz} is the HOMO−1, and π_1^* and π_2^* are the LUMO and LUMO+1, respectively. For the reasons discussed above the $\langle d_{yz}\rightarrow\pi_1^*|\hat{H}_{SO}|d_{yz}\rightarrow\pi_2^*\rangle$ and $\langle d_{xz}\rightarrow\pi_1^*|\hat{H}_{SO}|d_{xz}\rightarrow\pi_2^*\rangle$ integrals do not contribute.

We have recently reported[43] that for $[Cu(dmp)_2]^+$ efficient ISC occurs along the flattening coordinate where the S_1 state becomes degenerate with the T_2, T_3, and T_4 states. This occurs because the rate of ISC, related to the mixing between the singlet and triplet states is dependent not only on the SOC matrix elements but also on the gap between the two coupled states, as shown in eq 2. To assess this for $[Cu(dmdp)_2]^+$, Figure 2 shows the excited states and SOC matrix elements along its flattening coordinate. Importantly, the T_3 and T_4 states cross S_1 and S_2, and in conjunction with the significant coupling at the corresponding crossing points one could expect bifurcation of the wavepacket and ultrafast ISC as recently reported for $[Cu(dmp)_2]^+$.[43]

For complexes that exhibit a broken symmetry and a flattened dihedral angle in both the ground and lowest triplet states, the SOC matrix elements are significantly reduced, <50 cm^{-1}. This is because the main configurations for both the S_1 and T_1 states correspond to the $d_{yz} \rightarrow \pi^*$ transitions. Consequently, as these transitions do not involve any change in the d-orbital angular momentum, the SOC integrals work only between ligand-centered molecular orbitals instead of metal-centered ones. In this case, the small spin−orbit coupling constant of these elements means that no significant SOC matrix elements arise.

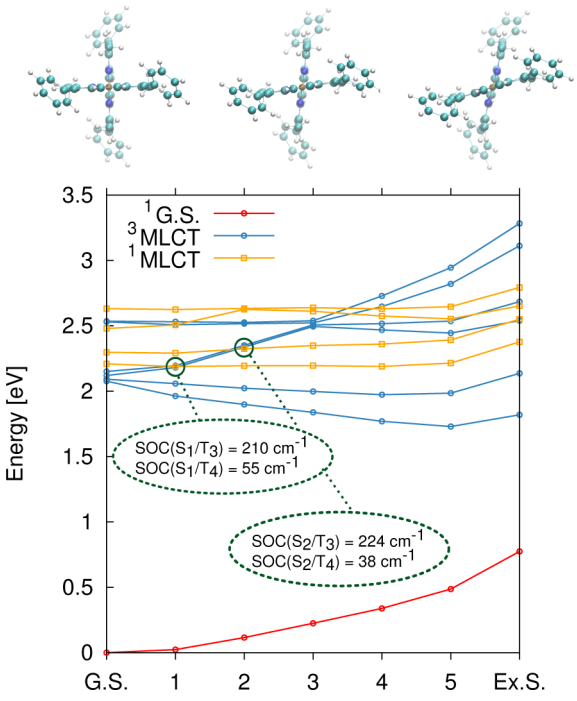

Figure 2. Energy, in eV, of the ground state (red) singlet (orange) and triplet (blue) MLCT excited state of $[Cu(dmdp)_2]^+$ along the coordinate that connects the ground and excited state geometries (principally the flattening of the ligands). Spin−orbit coupling elements, in cm^{-1}, between S_1 and S_2 with T_3 and T_4 are shown as well.

Molecular Dynamics: Role of the Solvent. In the previous sections we have focused on the influence of the electronic and structural properties on the luminescence characteristics. However, as outlined in the Introduction, the solvent is well documented to also play a crucial role in the luminescence lifetime of these complexes. In this subsection we present classical and QM/MM MD simulations, as described above, aimed at elucidating the exact nature of the solvent interaction.

Table 3 shows the mean values and standard deviations of the most relevant structural parameters obtained from the QM/MM and classical MD simulations. For the complexes computed with both methods ($[Cu(phen)_2]^+$, $[Cu(dpp)_2]^+$, $[Cu(dbp)_2]^+$), we find close agreement between these simulations and the gas phase optimizations shown in Table S2 (Supporting Information). This verifies the validity of the force fields and demonstrates that the solvent does not have an influence on the geometric structure of the complexes. However, there is one notable exception, namely, the dihedral angle between the ligands of $[Cu(dpp)_2]^+$ in both the ground and excited states. This difference is because the dihedral angle of the phenyl-substituted complexes is sensitive to the description of the weak $\pi-\pi$ stacking interactions. For this

DOI: 10.1021/acs.jpca.5b03842
J. Phys. Chem. A 2015, 119, 7026−7037

Table 3. Mean Values for Selected Geometrical Features with Corresponding Standard Deviations (σ) from the QM/MM and Classical Simulations (CMD)[a]

		ground state			^{3}MLCT		
	method	Cu−N (Å)	∠NCuN$_{intra}$ (deg)	∠DHA (deg)	Cu−N (Å)	∠NCuN$_{intra}$ (deg)	∠DHA (deg)
$[Cu(phen_2)]^+$	CMD	2.00 (0.066)	83 (2.6)	90 (9)	1.98 (0.035)	85 (1.4)	48 (7)
	QM/MM	2.03 (0.075)	83 (2.5)	82 (20)	2.01 (0.073)	83 (3.4)	41 (9)
$[Cu(tfp)_2]^+$	CMD	2.08 (0.062)	81 (2.5)	90 (7)	2.02 (0.036)	85 (1.5)	75 (7)
$[Cu(dmdp)_2]^+$	CMD	2.00 (0.065)	81 (2.6)	94 (11)	1.98 (0.036)	84 (1.6)	76 (7)
$[Cu(dpp)_2]^+$	CMD	2.02 (0.036)	85 (1.5)	55 (7)	1.95 (0.035)	89 (1.6)	51 (7)
	QM/MM	2.08 (0.091)	83 (2.8)	67 (9)	2.04 (0.086)	84 (3.1)	64 (12)
		2.03 (0.080)			2.01 (0.080)		
$[Cu(dpdmp)_2]^+$	CMD	2.01 (0.036)	85 (1.5)	54 (7)	1.95 (0.036)	88 (1.6)	52 (7)
$[Cu(dptmp)_2]^+$	CMD	2.01 (0.036)	85 (1.5)	65 (7)	1.95 (0.036)	88 (1.5)	65 (7)
$[Cu(tpp)_2]^+$	CMD	2.05 (0.036)	84 (1.5)	53 (7)	1.94 (0.036)	88 (1.6)	51 (7)
$[Cu(dbp)_2]^+$	CMD	2.04 (0.056)	81 (1.4)	87 (6)	2.02 (0.036)	83 (1.6)	74 (7)
					1.98 (0.036)	84 (1.6)	
	QM/MM	2.05 (0.087)	83 (2.7)	95 (10)	2.02 (0.081)	85 (2.7)	78 (11)
					2.00 (0.072)		
$[Cu(dbtmp)_2]^+$	CMD	2.05 (0.062)	81 (2.5)	90 (7)	2.02 (0.035)	84 (1.5)	77 (7)

[a]The Cu−N is the bond distance between the Copper and the four nitrogens of the phenanthrolines ligands. NCuN$_{intra}$ is the angle the copper makes with the two nitrogens atoms on the same phenanthroline ligand; DHA is the dihedral angle between the ligands.

complex, the force field is parametrized using DFT(BLYP) and incorporated the effect of the weak $\pi-\pi$ interactions through Grimme's D2 dispersion correction.[62] In contrast, for the QM/MM simulations, the $\pi-\pi$ interactions between the atoms in the QM subsystem were described using the dispersion-corrected atom-centered potential (DCACP)[82−84] method. Note that van der Waals interactions between the solute (DFT) and the solvent (force field) are treated at a classical level. This results in a larger, by ∼10°, dihedral angle in the case of the latter, which is in better agreement with previous experimental observations.[92,93] Importantly, an additional gas phase geometry optimization performed within CPMD using DCACP demonstrated that the difference arises solely from the description of the $\pi-\pi$ interactions and is not a structural change induced by the solvent shell. However, as demonstrated in Figure S6 (Supporting Information), this difference in the dihedral angle does not have a significant effect on the structure of the first solvation shell in the ground state. Though, as a consequence of this large dihedral angle in the classical MD simulations, a slightly stronger solute−solvent interaction is observed in the excited state, this does not change the qualitative interpretation of the results as discussed below.

Figures 3−5 show the Cu−N$_{MeCN}$ and Cu−Cl$_{DCM}$ radial distribution functions (RDF) and distance dependent coordination number, $N(r)$, for both the ground (GS) and excited states (ES) extracted from the classical MD simulations. For $[Cu(phen_2)]^+$, $[Cu(dpp)_2]^+$, and $[Cu(dbp)_2]^+$ these are compared to the RDFs obtained from the QM/MM MD configurations in Figures S5−S7 (Supporting Information). These show good agreement between the solvent structure for the two simulations up to 10 Å from the copper ion.

The red trace in Figure 3 corresponds to the solvation structure of $[Cu(phen)_2]^+$. As this complex has no substituents on the phenanthroline ligands, it is expected to exhibit the largest interaction with the solvent and, indeed, this is observed for both the ground and excited states. For the complex dissolved in MeCN, the first Cu−N$_{MeCN}$ solvation shell peak in both the ground and excited states is observed at ∼4 Å. However, in both cases this solvent shell does not form a distinct structure separated from the bulk solvent, and the RDF

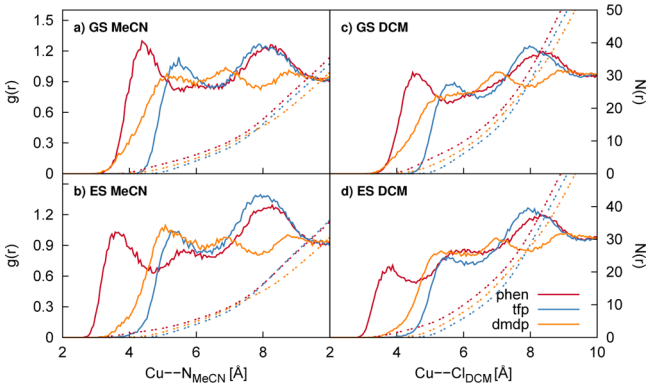

Figure 3. Radial distribution function $g(r)$ and integrated radial distribution function $N(r)$ extracted from the classical MD of $[Cu(phen)_2]^+$, $[Cu(tfp)_2]^+$, and $[Cu(dmdp)_2]^+$ in the ground state for MeCN (a) and DCM (c) and the lowest triplet excited state for MeCN (b) and DCM (d).

indicates continuous exchange between the first solvation shell and the rest of the solvent. This is accentuated in the excited state. Therefore, although due to the large flattening angle there is likely to be a solvent interaction at the Cu ion, this is weak (r > 3 Å) and leads to a transient structure that cannot be defined an as exciplex. The RDF for the complex dissolved in DCM (Figure 3c,d) shows that the solvent molecules are able to come slightly closer to the copper ion. In this case, the very large dihedral angle in the excited state introduces no steric hindrance for either the chlorine or nitrogen atoms, providing therefore the optimal conditions for the direct interaction of the metal ion with the solvent. However, also in this case we do not observe the formation of an exciplex. This would appear to rule out the possibility of a direct solvent effect on the lifetime of $[Cu(phen)_2]^+$ occurring at the copper ion. Recently, Hua et al.[41] reported that the principal luminescence from $[Cu(phen)_2]^+$ occurs from the lowest singlet excited state and has a lifetime of 1.8 ps in DCM and 1.4 ps in MeCN. The authors attributed this small quenching to stabilization of the charge transfer character state in a more polar solvent. This is

DOI: 10.1021/acs.jpca.5b03842
J. Phys. Chem. A 2015, 119, 7026−7037

consistent with our present simulations, as this assignment is an outer-sphere effect and therefore is not influenced by the Cu−solvent interaction distances. It is worth noting that there appears to be a distinct difference in the total lifetime of $[Cu(phen)_2]^+$ in DCM reported in ref 41 and by Chen et al.[94] This difference occurs as the former does not include the small fraction of phosphorescence ($\Phi \sim 0.1$) arising from a fraction of the wavepacket that undergoes intersystem crossing (ISC). Interestingly, in ref 41 ISC is not observed when the complex is dissolved in MeCN. Due to the lifetime of the excited state and small SOC, this fraction of ISC cannot occur in S_1 at the flattened geometry and therefore must occur along the flattening coordinate where the low-lying triplets are degenerate with the S_1 state, as recently proposed from high-level quantum dynamics simulations.[43] Consequently, ISC is observed for DCM and not MeCN as the higher viscosity of the solvent leads to the wavepacket taking longer (~0.1 ps) to traverse the flattening coordinate where the probability of ISC is higher.

The effect of the addition of small substituents, CF_3 ($[Cu(tfp)_2]^+$) and CH_3 ($[Cu(dmdp)_2]^+$), in the 2,9 position of the phenanthroline ligands are shown in Figure 3. In both cases the first solvation shell shifts further away from copper, as expected. However, although the peak of the first solvation shells appear at similar distances, the additional steric hindrance of the fluorine atoms, in comparison to the case for the hydrogens, means that there is a smaller probability for the solvent molecules to come close (<4 Å) to the Cu ion. The other significant effect is that of the phenyl groups in the 4,7 positions of $[Cu(dmdp)_2]^+$, which pushes the outer-sphere solvent molecules further away from the core of the phenanthroline ligands as demonstrated by the loss of the peak in the RDF at ~8 Å.

Figure 4 shows the effect of adding phenyl ligands in the 2,9 positions of the phenanthroline ligands. When compared with

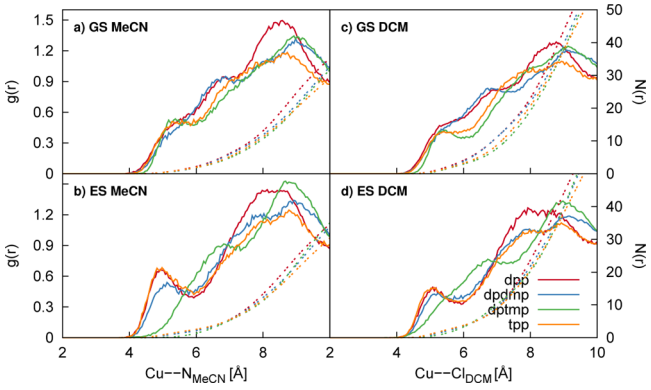

Figure 4. Radial distribution function $g(r)$ and integrated radial distribution function $N(r)$ extracted from the classical MD of $[Cu(dpp)_2]^+$, $[Cu(dpdmp)_2]^+$, $[Cu(dptmp)_2]^+$ and $[Cu(tpp)_2]^+$ in the ground state for MeCN (a) and DCM (c) and the lowest triplet excited state for MeCN (b) and DCM (d).

the radial distribution profiles obtained for the complexes with small substituents (Figure 3), several important differences are observed. The first solvation peak around ~5 Å is strongly reduced, and the overall profile becomes less structured. Indeed, the main feature in the RDF does not occur until between 8 and 10 Å away from the copper. We also observe much smaller changes between the ground and the excited state solvent structures, consistent with the small changes in the solute.

Finally, Figure 5 shows the effect of adding alkyl substituents in the 2,9 position of the phenanthrolines ligands. Like for the

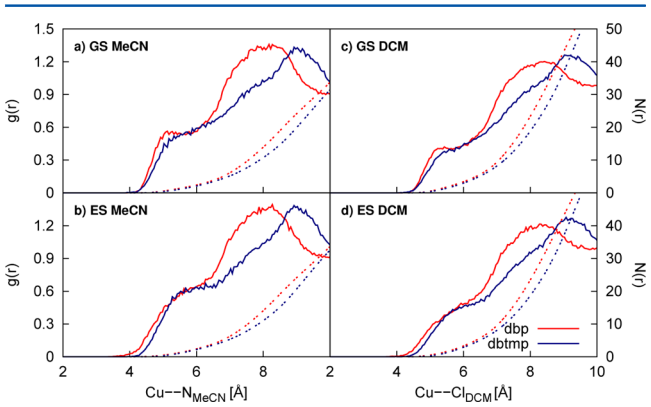

Figure 5. Radial distribution function $g(r)$ and integrated radial distribution function $N(r)$ extracted from the classical MD of $[Cu(dbp)_2]^+$ and $[Cu(dbtmp)_2]^+$ in the ground state for MeCN (a) and DCM (c) and the lowest triplet excited state for MeCN (b) and DCM (d).

phenyl substituents, these significantly reduce the magnitude of the first solvation shell. Again, the substituents pointing toward the bulk have only a very small effect at short distances (<6 Å). This effect is larger at <6 Å and is associated with the second solvation shell being shifted outward. Although this will reduce the interaction between the solvent and the complex, it is expected to have very little effect on the lifetime arising from solvent interactions.

Though useful, the RDFs presented in the previous section do not contain information about the angular distribution of the solvent shell. Figure 6 shows the solvent density around the $[Cu(phen)_2]^+$, $[Cu(dpp)_2]^+$, and $[Cu(dbp)_2]^+$. Corresponding plots for the other complexes are shown in Figures S8−13 (Supporting Information). For $[Cu(phen)_2]^+$, we find an ordered first solvation shell, which follows and intercalates along the lines of the phenanthroline ligands in a manner similar to that reported for $[Ru(bpy)_3]^{2+}$ [95,96] and $[Fe(bpy)_3]^{2+}$.[97,98] Importantly, as indicated by the RDFs, the solvent structure does not change significantly in the excited state, indicating that although a weak solvent effect is present in the excited state, it does not arise from a particular solvent structure. Importantly, although this order is retained, to a certain extent, with phenyl and alkyl groups substituted into the 2,9 positions, these plots clearly show a distant disruption of the first solvation shell, especially in the case of the latter. This increased disorder in the solvent structure is likely correlated to a decrease of the solvent induced effects on the ground and excited state dynamics.

DISCUSSIONS AND CONCLUSIONS

The photophysical properties of the Cu(I)−phenanthroline complexes have drawn significant attention owing to a range of possible applications and have been widely studied as prototypical mononuclear Cu(I) complexes. In the previous sections we have presented detailed simulations aimed at providing a comprehensive description of the role of the electronic and geometric structure, the SOC, and solvent environment in determining the luminescent properties. In this

DOI: 10.1021/acs.jpca.5b03842
J. Phys. Chem. A 2015, 119, 7026−7037

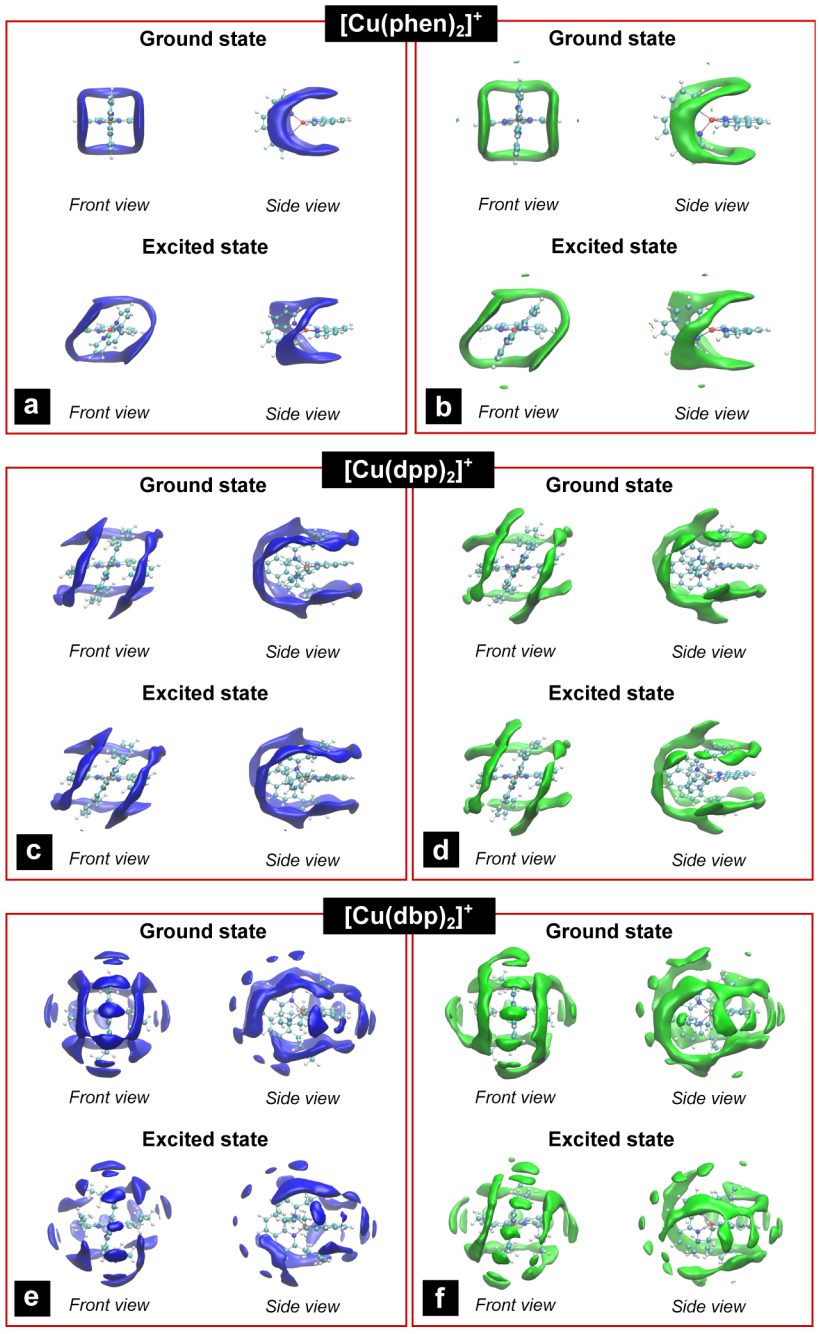

Figure 6. Solvent density of MeCN (blue) and DCM (green) around $[Cu(phen)_2]^+$, $[Cu(dpp)_2]^+$, and $[Cu(dbp)_2]^+$, in both the ground and ^{3}MLCT state.

section we discuss the implications of these results and possible pathways to further develop their applicability.

In the first section of our present study we performed quantum chemistry calculations to rationalize the effect of ligand modifications on the emission properties and lifetime of these complexes and have observed a number of trends. First, the energy gap between the ground and excited states, crucial in terms of the contribution of nonradiative relaxations is strongly dependent on the dihedral angle between the ligands, and consequently, to maintain a significant radiative emission by virtue of the large energy gap, these structural distortions must be minimized. Indeed, one effective way to control this is including methyl substituents in the 3,8 positions. Here the steric hindrance with the substituents in the 2,9 position, reduces the flattening distortion in the excited states and can significantly extend the excited state lifetime.[87] Second, the $S_1 \rightarrow S_0$ oscillator strength is strongly dependent on the ligand substitutions on the phenanthroline ligands. If the π system of the ligands is pushed toward the Cu center, i.e., with phenyl substituents in the 2,9 positions, the dipole length is reduced, decreasing the oscillator strength. As expected, the opposite is observed if phenyl substituents are used in the 4,7 positions. The inductive effect of the alkyl substituents leads to the opposite trends when in the same position. Third, the emission from the triplet state also has a strong bearing on the emission. This gains intensity through mixing with the lowest singlet states and is dependent upon both the energy gap between the state sand the SOC matrix elements. For the former,

DOI: 10.1021/acs.jpca.5b03842
J. Phys. Chem. A 2015, 119, 7026−7037

delocalization of the unoccupied orbitals, populated upon excitation by for instance phenyl substituents in the 4,7 positions, decreases the energy gaps between the singlet and triplet state by virtue of a reduced exchange interaction. This increases the mixing of the singlet and triplet state making the radiative rate from the triplet state large reducing the excited state lifetime.

To assess the role and factors affecting the SOC within these complexes, we have performed SOC-TDDFT calculations as described. In agreement with the semiquantitative study performed by Siddique et al.[88] on $[Cu(dmp)_2]^+$, we find that the magnitude of spin−orbit coupling matrix elements are dependent almost exclusively upon the dihedral angle between the ligands. This arises from an *internal effect* associated with the changing character, of the excited states, especially that of the Cu d-orbitals, upon flattening of the dihedral angle. Indeed, when the two ligands are perpendicular (or close to), the D_{2d} symmetry means that the d_{xz} and d_{yz} orbitals are degenerate and consequently both contribute to the character of the low-lying excited states. This provides an effective mechanism for spin−orbit coupling, as the one-center SOC integral between these orbitals fulfills at best the total angular momentum conservation rule. However, flattening of the dihedral angle disfavors the transition between the d_{xy} and d_{yz} orbitals. As a consequence, the SOC matrix elements acquires intensity only through the coupling of ligand-centered molecular orbitals and are small due to the absence of heavy elements.

Using classical and QM/MM molecular dynamics, we have provided a detailed study of the exact nature of the solvation shell around these complexes in both the ground and lowest triplet excited states. In agreement with out recent time-resolved X-ray absorption study,[50] these simulations demonstrate that the lifetime shortening of the excited state in donor solvents (acetonitrile) is not due to the formation of an exciplex. Instead, although the solute−solvent interaction still occurs at the metal center it is weak and therefore transient in nature. Crucially, this arises from a solvent structure already present in the electronic ground state. Indeed, even for $[Cu(phen)_2]^+$ that has no substituents on the phenanthroline ligands and therefore would be expected to exhibit the largest interaction with the solvent, the solvation structure of the closest solvent molecules in both the ground and excited states is observed at ∼3 Å. But, in both cases this solvent structure is not a distinct structure separated from the bulk solvent and undergoes continual exchange between the first solvation shell and the rest of the solvent. The solvent structure extracted from the molecular dynamics simulations shows that all substituents larger than CH_3 prevent the solvent molecules from coming closer than ∼4 Å to the Cu ion. Crucially, in terms of preventing the solvent effect, this therefore does not provide a large restriction on the choice of ligands required in the 2,9 positions of the phenanthroline ligands.

In conclusion, using DFT, TDDFT, and classical and QM/MM MD simulations, we have elucidated the role of the geometric and electronic structure, spin−orbit coupling, singlet−triplet gap, and the solvent environment on the emission properties of nine prototypical copper(I)−phenanthroline complexes. In terms of future studies, it is worth noting that this study has focused on the homoleptic complexes. However, the general principles discussed are certainly applicable to hetreoleptic complexes that have also been explored for TADF emitter in OLEDS.[99] Indeed, these complexes offer great potential due to the multitude of possible variations of the involved ligands, and although additional care has been taken due to their thermodynamic stability,[100] recent work has demonstrated that such complexes can exhibit promising device performance.[101]

■ ASSOCIATED CONTENT

Supporting Information

Structure with ligand nomenclature; discussions of the geometric structure, absorption characteristics, and classical molecular dynamics; tables of emission lifetimes, optimized geometries, absorption data, force field parameters, and Cartesian coordinates; figures of compaison of thermal distributions, RDFs, and solvent densities. The Supporting Information is available free of charge on the ACS Publications website at DOI: 10.1021/acs.jpca.5b03842.

■ AUTHOR INFORMATION

Corresponding Author

*T. J. Penfold. E-mail: tom.penfold@ncl.ac.uk.

Notes

The authors declare no competing financial interest.

■ ACKNOWLEDGMENTS

We thank the Swiss National Science Foundation (Grant 200021-137717) and the NCCR MUST for funding.

■ REFERENCES

(1) Damrauer, N. H. Femtosecond Dynamics of Excited-State Evolution in [Ru(bpy)3]2+. *Science* **1997**, *275*, 54−57.

(2) Yeh, A. T. Ultrafast Electron Localization Dynamics Following Photo-Induced Charge Transfer. *Science* **2000**, *289*, 935−938.

(3) Bhasikuttan, A. C.; Suzuki, M.; Nakashima, S.; Okada, T. Ultrafast Fluorescence Detection in Tris(2,2′-bipyridine)ruthenium(II) Complex in Solution: Relaxation Dynamics Involving Higher Excited States. *J. Am. Chem. Soc.* **2002**, *124*, 8398−8405.

(4) Cannizzo, A.; van Mourik, F.; Gawelda, W.; Zgrablic, G.; Bressler, C.; Chergui, M. Broadband Femtosecond Fluorescence Spectroscopy of $[Ru(bpy)_3]^{2+}$. *Angew. Chem., Int. Ed.* **2006**, *45*, 3174−3176.

(5) Tavernelli, I.; Curchod, B.; Rothlisberger, U. Nonadiabatic Molecular Dynamics with Solvent Effects: A LR-TDDFT QM/MM Study of Ruthenium (II) tris (bipyridine) in Water. *Chem. Phys.* **2011**, *391*, 101−109.

(6) Juris, A.; Balzani, V.; Barigelletti, F.; Campagna, S.; Belser, P.; von Zelewsky, A. Ru(II) Polypyridine Complexes: Photophysics, Photochemistry, Eletrochemistry, and Chemiluminescence. *Coord. Chem. Rev.* **1988**, *84*, 85−277.

(7) el Nahhas, A.; Cannizzo, A.; van Mourik, F.; Blanco-Rodriguez, A. M.; Zalis, S.; Vlcek, A. J.; Chergui, M. Ultrafast Excited-State Dynamics ef [Re(L)(CO)(3)(bpy)](n) Complexes: Involvement of the Solvent. *J. Phys. Chem. A* **2010**, *114*, 6361−6369.

(8) el Nahhas, A.; et al. Ultrafast Excited-State Dynamics of Rhenium(I) Photosensitizers [Re(Cl)(CO)(3)(N,N)] and [Re(imidazole)(CO)(3)(N,N)](+): Diimine Effects. *Inorg. Chem.* **2011**, *50*, 2932−2943.

(9) el Nahhas, A.; et al. X-ray Absorption Spectroscopy of Ground and Excited Rhenium-Carbonyl-Diimine Complexes: Evidence for a Two-Center Electron Transfer. *J. Phys. Chem. A* **2013**, *117*, 361−369.

(10) Cannizzo, A.; Blanco-Rodriguez, A. M.; El Nahhas, A.; Sebera, J.; Zalis, S.; Vlcek, A., Jr.; Chergui, M. Femtosecond Fluorescence and Intersystem Crossing in Rhenium (I) Carbonyl- Bipyridine Complexes. *J. Am. Chem. Soc.* **2008**, *130*, 8967−8974.

(11) Vlček, A., Jr *Photophysics of Organometallics*; Springer: Berlin, 2010; pp 115−158.

(12) Braem, O.; Messina, F.; Baranoff, E.; Cannizzo, A.; Nazeeruddin, M. K.; Chergui, M. Ultrafast Relaxation Dynamics of Osmium-

Polypyridine Complexes in Solution. *J. Phys. Chem. C* **2013**, *117*, 15958−15966.
(13) Zhang, X.; et al. Highly Accurate Excited-State Structure of [Os(bpy)2dcbpy] 2+ Determined by X-ray Transient Absorption Spectroscopy. *J. Am. Chem. Soc.* **2014**, *136*, 8804−8809.
(14) Fleming, C. N.; Maxwell, K. A.; DeSimone, J. M.; Meyer, T. J.; Papanikolas, J. M. Ultrafast Excited-State Energy Migration Dynamics in an Efficient Light Harvesting Antenna Polymer based on Ru (II) and Os (II) Polypyridyl Complexes. *J. Am. Chem. Soc.* **2001**, *123*, 10336−10347.
(15) Shaw, G. B.; Styers-Barnett, D. J.; Gannon, E. Z.; Granger, J. C.; Papanikolas, J. M. Interligand Electron Transfer Dynamics in [Os (bpy) 3] 2+: Exploring the Excited State Potential Surfaces with Femtosecond Spectroscopy. *J. Phys. Chem. A* **2004**, *108*, 4998−5006.
(16) Castellano, F. N.; Pomestchenko, I. E.; Shikhova, E.; Hua, F.; Muro, M. L.; Rajapakse, N. Photophysics in Bipyridyl and Terpyridyl Platinum (II) Acetylides. *Coord. Chem. Rev.* **2006**, *250*, 1819−1828.
(17) Rachford, A. A.; Goeb, S.; Ziessel, R.; Castellano, F. N. Ligand Localized Triplet Excited States in Platinum (II) Bipyridyl and Terpyridyl Peryleneacetylides. *Inorg. Chem.* **2008**, *47*, 4348−4355.
(18) Zhao, N.; Wu, Y.-H.; Wen, H.-M.; Zhang, X.; Chen, Z.-N. Conversion from ILCT to LLCT/MLCT Excited State by Heavy Metal Ion Binding in Iridium (III) Complexes with Functionalized 2,2-bipyridyl Ligands. *Organometallics* **2009**, *28*, 5603−5611.
(19) Yang, C.-H.; Li, S.-W.; Chi, Y.; Cheng, Y.-M.; Yeh, Y.-S.; Chou, P.-T.; Lee, G.-H.; Wang, C.-H.; Shu, C.-F. Heteroleptic Cyclometalated Iridium (III) Complexes Displaying Blue Phosphorescence in Solution and Solid State at Room Temperature. *Inorg. Chem.* **2005**, *44*, 7770−7780.
(20) Li, J.; Djurovich, P. I.; Alleyne, B. D.; Yousufuddin, M.; Ho, N. N.; Thomas, J. C.; Peters, J. C.; Bau, R.; Thompson, M. E. Synthetic Control of Excited State Properties in Cyclometalated Ir (III) Complexes Using Ancillary Ligands. *Inorg. Chem.* **2005**, *44*, 1713−1727.
(21) Yersin, H. *Highly efficient OLEDs with Phosphorescent Materials*; John Wiley & Sons: New York, 2008.
(22) Kafafi, Z. H. *Organic electroluminescence*; CRC Press: Boca Raton, FL, 2005.
(23) Shinar, J.; Savvateev, V. *Introduction to Organic Light-Emitting Devices*; Springer: Berlin, 2004.
(24) Su, H.-C.; Chen, H.-F.; Fang, F.-C.; Liu, C.-C.; Wu, C.-C.; Wong, K.-T.; Liu, Y.-H.; Peng, S.-M. Solid State White Light-Emitting Electrochemical Cells using Iridium Based Cationic Transition Metal Complexes. *J. Am. Chem. Soc.* **2008**, *130*, 3413−3419.
(25) Slinker, J.; Bernards, D.; Houston, P.; Abruna, H.; Bernhard, S.; Malliaras, G. Solid State Electroluminescent Devices Based on Transition Metal Complexes. *Chem. Commun.* **2003**, *9*, 2392−2399.
(26) Zhao, Q.; Li, F.; Huang, C. Phosphorescent Chemosensors Based on Heavy Metal Complexes. *Chem. Soc. Rev.* **2010**, *39*, 3007−3030.
(27) Keefe, M.; Benkstein, K.; Hupp, J. Luminescent Sensor Molecules Based on Coordinated Metals: A Review of Recent Developments. *Coord. Chem. Rev.* **2000**, *205*, 201−228.
(28) Baggaley, E.; Weinstein, J. A.; Williams, J. A. Lighting the Way to See Inside the Live Cell with Luminescent Transition Metal Complexes. *Coord. Chem. Rev.* **2012**, *256*, 1762−1785.
(29) Lawthers, I.; McGarvey, J. J. Spin State Relaxation Dynamics in Iron (III) Complexes: Photochemical Perturbation of the 2T→ 6A Spin Equilibrium by Pulsed Laser Irradiation in the Ligand-to-Metal Charge-Transfer Absorption Band. *J. Am. Chem. Soc.* **1984**, *106*, 4280−4282.
(30) Cannizzo, A.; Milne, C.; Consani, C.; Gawelda, W.; Bressler, C.; van Mourik, F.; Chergui, M. Light Induced Spin Crossover in Fe (II)-based Complexes: The Full Photocycle Unraveled by Ultrafast Optical and X-ray Spectroscopies. *Coord. Chem. Rev.* **2010**, *254*, 2677−2686.
(31) Fredin, L. A.; Pápai, M.; Rozsályi, E.; Vanko, G.; Wärnmark, K.; Sundström, V.; Persson, P. Exceptional Excited-State Lifetime of an Iron(II)-N-Heterocyclic Carbene Complex Explained. *J. Phys. Chem. Lett.* **2014**, *5*, 2066−2071.
(32) Visbal, R.; Gimeno, M. C. N-Heterocyclic Carbene Metal Complexes: Photoluminescence and Applications. *Chem. Soc. Rev.* **2014**, *43*, 3551−3574.
(33) Barbieri, A.; Accorsi, G.; Armaroli, N. Luminescent Complexes Beyond the Platinum Group: The d10 Avenue. *Chem. Commun.* **2008**, *19*, 2185−2193.
(34) Armaroli, N. Photoactive mono- and polynuclear Cu(I)-Phenanthrolines. A Viable Alternative to Ru(II)-Polypyridines? *Chem. Soc. Rev.* **2001**, *30*, 113−124.
(35) Lazorski, M. S.; Castellano, F. N. Advances in the Light Conversion Properties of Cu (I)-Based Photosensitizers. *Polyhedron* **2014**, *82*, 57−70.
(36) Shaw, G. B.; Grant, C. D.; Shirota, H.; Castner, E. W.; Meyer, G. J.; Chen, L. X. Ultrafast Structural Rearrangements in the MLCT Excited State for Copper(I) bis-Phenanthrolines in Solution. *J. Am. Chem. Soc.* **2007**, *129*, 2147−2160.
(37) Chen, L. X.; Zhang, X.; Lockard, J. V.; Stickrath, A. B.; Attenkofer, K.; Jennings, G.; Liu, D.-J. Excited State Molecular Structures Captured by X-ray Transient Absorption Spectroscopy: A Decade and Beyond. *Acta Crystallogr., Sect. A: Found. Crystallogr.* **2010**, *66*, 240−251.
(38) Iwamura, M.; Ishii, K.; Takeuchi, S.; Tahara, T. Real-time Observation of the Photoinduced Structural Change of Bis(2,9-dimethyl-1,10-Phenanthroline)copper(I) by Femtosecond Fluorescence Spectroscopy: A Realistic Potential Curve of the Jahn-Teller Distortion. *J. Am. Chem. Soc.* **2007**, *129*, 5248−5256.
(39) Iwamura, M.; Watanabe, H.; Ishii, K.; Takeuchi, S.; Tahara, T. Coherent Nuclear Dynamics in Ultrafast Photoinduced Structural Change of Bis(diimine)copper(I) Complex. *J. Am. Chem. Soc.* **2011**, *133*, 7728−7736.
(40) Iwamura, M.; Takeuchi, S.; Tahara, T. Substituent Effect on the Photoinduced Structural Change of Cu(I) Complexes Observed by Femtosecond Emission Spectroscopy. *Phys. Chem. Chem. Phys.* **2014**, *16*, 4143−4154.
(41) Hua, L.; Iwamura, M.; Takeuchi, S.; Tahara, T. The Substituent Effect on the MLCT Excited State Dynamics of Cu(i) Complexes Studied by Femtosecond Time-Resolved Absorption and Observation of Coherent Nuclear Wavepacket Motion. *Phys. Chem. Chem. Phys.* **2015**, *17*, 2067−2077.
(42) Capano, G.; Penfold, T. J.; Rothlisberger, U.; Tavernelli, I. A Vibronic Coupling Hamiltonian to Describe the Ultrafast Excited State Dynamics of a Cu(I)-Phenanthroline Complex. *Chimia* **2014**, *68*, 227−230.
(43) Capano, G.; Chergui, M.; Rothlisberger, U.; Tavernelli, I.; Penfold, T. J. A Quantum Dynamics Study of the Ultrafast Relaxation in a Prototypical Cu(I)-Phenanthroline. *J. Phys. Chem. A* **2014**, *118*, 9861−9869.
(44) McMillin, D. R.; Kirchhoff, J. R.; Goodwin, K. V. Exciplex Quenching of Photoexcited Copper Complexes. *Coord. Chem. Rev.* **1985**, *64*, 83−92.
(45) Blaskie, M. W.; McMillin, D. R. Photostudies of Copper(I) Systems. 6. Room-Temperature Emission and Quenching Studies of Bis(2,9-dimethyl-1,10-phenanthroline)copper(I). *Inorg. Chem.* **1980**, *19*, 3519−3522.
(46) del Paggio, A. A.; McMillin, D. R. Substituent Effects and the Photoluminescence of Cu(PPh3)2(NN)+ Systems. *Inorg. Chem.* **1983**, *22*, 691−692.
(47) Scaltrito, D.; Thompson, D.; O'Callaghan, J.; Meyer, G. MLCT Excited States of Cuprous Bis-Phenanthroline Coordination Compounds. *Coord. Chem. Rev.* **2000**, *208*, 243−266.
(48) Eggleston, M. K.; McMillin, D. R.; Koenig, K. S.; Pallenberg, A. J. Steric Effects in the Ground and Excited States of Cu (NN) 2+ Systems. *Inorg. Chem.* **1997**, *36*, 172−176.
(49) Englman, R.; Jortner, J. The Energy Gap Law for Radiationless Transitions in Large Molecules. *Mol. Phys.* **1970**, *18*, 145−164.
(50) Penfold, T. J.; Karlsson, S.; Capano, G.; Lima, F. A.; Rittmann, J.; Reinhard, M.; Rittmann-Frank, M. H.; Braem, O.; Baranoff, E.; Abela, R.; et al. Solvent-Induced Luminescence Quenching: Static and

DOI: 10.1021/acs.jpca.5b03842
J. Phys. Chem. A 2015, 119, 7026−7037

Time-Resolved X-Ray Absorption Spectroscopy of a Copper(I) Phenanthroline Complex. *J. Phys. Chem. A* **2013**, *117*, 4591−4601.
(51) Milne, C.; Penfold, T.; Chergui, M. Recent Experimental and Theoretical Developments in Time-Resolved X-ray Spectroscopies. *Coord. Chem. Rev.* **2014**, *277*, 44−68.
(52) Reinhard, M.; Penfold, T. J.; Lima, F. A.; Rittmann, J.; Rittmann-Frank, M. H.; Abela, R.; Tavernelli, I.; Rothlisberger, U.; Milne, C. J.; Chergui, M. Photooxidation and Photoaquation of Iron Hexacyanide in Aqueous Solution: A Picosecond X-ray Absorption Study. *Struct. Dyn.* **2014**, *1*, 024901.
(53) Kirchhoff, J.; Gamache, R., Jr; Blaskie, M.; del Paggio, A.; Lengel, R.; McMillin, D. Temperature Dependence of Luminescence from Cu (NN) 2+ Systems in Fluid Solution. Evidence for the Participation of Two Excited States. *Inorg. Chem.* **1983**, *22*, 2380−2384.
(54) Zhang, Q.; Li, J.; Shizu, K.; Huang, S.; Hirata, S.; Miyazaki, H.; Adachi, C. Design of Efficient Thermally Activated Delayed Fluorescence Materials for Pure Blue Organic Light Emitting Diodes. *J. Am. Chem. Soc.* **2012**, *134*, 14706−14709.
(55) Czerwieniec, R.; Yu, J.; Yersin, H. Blue Light Emission of Cu (I) Complexes and Singlet Harvesting. *Inorg. Chem.* **2011**, *50*, 8293−8301.
(56) Penfold, T. J. On Predicting the Excited State Properties of Thermally Activated Delayed Fluorescence Emitters. *J. Phys. Chem. C* **2015**, *119*, 13535.
(57) Volz, D.; Wallesch, M.; Flechon, C.; Danz, M.; Verma, A.; Navarro, J. M.; Daniel, Z.; Braese, S.; Baumann, T. From Iridium and Platinum to Copper and Carbon: New Avenues for More Sustainability in organic Light Emitting Diodes. *Green Chem.* **2015**, *17*, 1988−2011.
(58) Lee, C.; Yang, W.; Parr, R. G. Development of the Colle-Salvetti Correlation- Energy Formula into a Functional of the Electron Density. *Phys. Rev. B: Condens. Matter Mater. Phys.* **1988**, *37*, 785−789.
(59) Becke, A. Density-Functional Exchange-Energy Approximation with Correct Asymptotic Behavior. *Phys. Rev. A: At., Mol., Opt. Phys.* **1988**, *38*, 3098−3100.
(60) Stephens, P. J.; Devlin, F. J.; Chabalowski, C. F.; Frisch, M. J. Ab Initio Calculation of Vibrational Absorption and Circular Dichroism Spectra Using Density Functional Force Fields. *J. Phys. Chem.* **1994**, *98*, 11623−11627.
(61) Frisch, M. J.; et al. *Gaussian 09*, Revision A.1; Gaussian Inc.: Wallingford, CT, 2009.
(62) Grimme, S. Semiempirical GGA-Type Density Functional Constructed with a Long-Range Dispersion Correction. *J. Comput. Chem.* **2006**, *27*, 1787.
(63) Fonseca Guerra, C.; Snijders, J. G.; te Velde, G.; Baerends, E. J. Towards an order-N DFT method. *Theor. Chem. Acc.* **1998**, *99*, 391−403.
(64) van Gisbergen, S.; Snijders, J.; Baerends, E. Implementation of Time-Dependent Density Functional Response Equations. *Comput. Phys. Commun.* **1999**, *118*, 119−138.
(65) *ADF2009.01, SCM*; Theoretical Chemistry, Vrije Universiteit, Amsterdam, The Netherlands, Scientific Computation and Modelling, 2010; http://www.scm.com/.
(66) Wang, F.; Ziegler, T. A Simplified Relativistic Time Dependent Density Functional Theory Formalism for the Calculations of Excitation Energies Including Spin-Orbit Coupling Effect. *J. Chem. Phys.* **2005**, *123*, 154102.
(67) Lenthe, E. v.; Baerends, E. J.; Snijders, J. G. Relativistic Regular Two-Component Hamiltonians. *J. Chem. Phys.* **1993**, *99*, 4597−4610.
(68) van Lenthe, E.; Baerends, E. J.; Snijders, J. G. Relativistic Total Energy using Regular Approximations. *J. Chem. Phys.* **1994**, *101*, 9783.
(69) Case, D. A.; et al. *AMBER 12*; University of California, San Francisco, 2012.
(70) Bayly, C. I.; Cieplak, P.; Cornell, W.; Kollman, P. A. A Well-Behaved Electrostatic Potential Based Method Using Charge Restraints For Deriving Atomic Charges: The RESP Model. *J. Phys. Chem.* **1993**, *97*, 10269−10280.
(71) Ichinaga, A. K.; Kirchhoff, J. R.; McMillin, D. R.; Dietrich-Buchecker, C. O.; Marnot, P. A.; Sauvage, J. P. Charge-Transfer Absorption and Emission of Cu (NN) 2+ Systems. *Inorg. Chem.* **1987**, *26*, 4290−4292.
(72) Cunningham, C. T.; Cunningham, K. L. H.; Michalec, J. F.; McMillin, D. R. Cooperative Substituent Effects on the Excited States of Copper Phenanthrolines. *Inorg. Chem.* **1999**, *38*, 4388−4392.
(73) Miller, M. T.; Gantzel, P. K.; Karpishin, T. B. A Photoluminescent Copper (I) Complex with an Exceptionally High CuII/CuI Redox Potential:[Cu (bfp) 2]+(bfp = 2,9-bis (trifluoromethyl)-1,10-phenanthroline. *Angew. Chem., Int. Ed.* **1998**, *37*, 1556−1558.
(74) Ruthkosky, M.; Castellano, F. N.; Meyer, G. J. Photodriven Electron and Energy Transfer from Copper Phenanthroline Excited States. *Inorg. Chem.* **1996**, *35*, 6406−6412.
(75) Car, R.; Parrinello, M. Unified Approach for Molecular Dynamics and Density-Functional Theory. *Phys. Rev. Lett.* **1985**, *55*, 2471−2474.
(76) Laio, A.; VandeVondele, J.; Rothlisberger, U. A Hamiltonian Electrostatic Coupling Scheme for Hybrid Car-Parrinello Molecular Dynamics Simulations. *J. Chem. Phys.* **2002**, *116*, 6941−6947.
(77) Laio, A.; VandeVondele, J.; Rothlisberger, U. D-RESP: Dynamically Generated Electrostatic Potential Derived Charges from Quantum Mechanics/Molecular Mechanics Simulations. *J. Phys. Chem. B* **2002**, *106*, 7300−7307.
(78) *CPMD*; Copyright IBM Corp 1990−2001, Copyright MPI für Festkörperforschung Stuttgart, 1997−2001; http://www.cpmd.org.
(79) Nose, S. A. Unified Formulation of the Constant Temperature Molecular-Dynamics Methods. *J. Chem. Phys.* **1984**, *81*, 511−519.
(80) Hoover, W. Canonical dynamics: Equilibrium Phase-Space Distributions. *Phys. Rev. A: At., Mol., Opt. Phys.* **1985**, *31*, 1695−1697.
(81) Troullier, N.; Martins, J. Efficient Pseudopotentials for Plane-Wave Calculations. *Phys. Rev. B: Condens. Matter Mater. Phys.* **1991**, *43*, 1993−2006.
(82) von Lilienfeld, O.; Tavernelli, I.; Rothlisberger, U.; Sebastiani, D. Optimization of Effective Atom Centered Potentials for London Dispersion Forces in Density Functional Theory. *Phys. Rev. Lett.* **2004**, *93*, 153004.
(83) von Lilienfeld, O.; Tavernelli, I.; Rothlisberger, U.; Sebastiani, D. Performance of Optimized Atom-Centered Potentials for Weakly Bonded Systems using Density Functional Theory. *Phys. Rev. B: Condens. Matter Mater. Phys.* **2005**, *71*, 195119.
(84) Lin, I.-C.; Coutinho-Neto, M.; Felsenheimer, C.; von Lilienfeld, O.; Tavernelli, I.; Rothlisberger, U. Library of Dispersion-Corrected Atom-Centered Potentials for Generalized Gradient Approximation Functionals: Elements H, C, N, O, He, Ne, Ar, and Kr. *Phys. Rev. B: Condens. Matter Mater. Phys.* **2007**, *75*, 205131.
(85) Phifer, C. C.; McMillin, D. R. The Basis of Aryl Substituent Effects on Charge-Transfer Absorption Intensities. *Inorg. Chem.* **1986**, *25*, 1329−1333.
(86) Endo, A.; Ogasawara, M.; Takahashi, A.; Yokoyama, D.; Kato, Y.; Adachi, C. Thermally Activated Delayed Fluorescence from Sn4+-Porphyrin Complexes and Their Application to Organic Light Emitting Diodes - A Novel Mechanism for Electroluminescence. *Adv. Mater.* **2009**, *21*, 4802−4806.
(87) McCusker, C. E.; Castellano, F. N. Design of a Long-Lifetime, Earth-Abundant, Aqueous Compatible Cu (I) Photosensitizer Using Cooperative Steric Effects. *Inorg. Chem.* **2013**, *52*, 8114−8120.
(88) Siddique, Z. A.; Yamamoto, Y.; Ohno, T.; Nozaki, K. Structure-Dependent Photophysical Properties of Singlet and Triplet Metal-to-Ligand Charge Transfer States in Copper(I) Bis(diimine) Compounds. *Inorg. Chem.* **2003**, *42*, 6366−6378.
(89) El Sayed, M. A. Spin-Orbit Coupling and the Radiationless Processes in Nitrogen Heterocyclics. *J. Chem. Phys.* **1963**, *38*, 2834.
(90) Rausch, A.; Homeier, H.; Yersin, H. In *Photophysics of Organometallics*; Lees, A. J., Ed.; Topics in Organometallic Chemistry; Springer: Berlin Heidelberg, 2010; Vol. *29*, pp 193−235.
(91) Hsu, C.-W.; Lin, C.-C.; Chung, M.-W.; Chi, Y.; Lee, G.-H.; Chou, P.-T.; Chang, C.-H.; Chen, P.-Y. Systematic Investigation of the Metal-Structure Photophysics Relationship of Emissive d10-Complexes of Group 11 Elements: The Prospect of Application in Organic Light Emitting Devices. *J. Am. Chem. Soc.* **2011**, *133*, 12085−12099.

DOI: 10.1021/acs.jpca.5b03842
J. Phys. Chem. A 2015, 119, 7026−7037

(92) Mara, M. W.; Jackson, N. E.; Huang, J.; Stickrath, A. B.; Zhang, X.; Gothard, N. A.; Ratner, M. A.; Chen, L. X. Effects of Electronic and Nuclear Interactions on the Excited-State Properties and Structural Dynamics of Copper(I) Diimine Complexes. *J. Phys. Chem. B* **2013**, *117*, 1921−1931.
(93) Cunningham, C. T.; Moore, J. J.; Cunningham, K. L. H.; Fanwick, P. E.; McMillin, D. R. Structural and Photophysical Studies of Cu(NN)2+ Systems in the Solid State. Emission at Last from Complexes with Simple 1,10-Phenanthroline Ligands. *Inorg. Chem.* **2000**, *39*, 3638−3644.
(94) Lockard, J. V.; Kabehie, S.; Zink, J. I.; Smolentsev, G.; Soldatov, A.; Chen, L. Influence of Ligand Substitution on Excited State Structural Dynamics in Cu(I) Bisphenanthroline Complexes. *J. Phys. Chem. B* **2010**, *114*, 14521−14527.
(95) Moret, M.-E.; Tavernelli, I.; Rothlisberger, U. Combined QM/MM and Classical Molecular Dynamics Study of [Ru(bpy)(3)](2+) in Water. *J. Phys. Chem. B* **2009**, *113*, 7737−7744.
(96) Moret, M.-E.; Tavernelli, I.; Chergui, M.; Rothlisberger, U. Electron Localization Dynamics in the Triplet Excited State of [Ru(bpy)(3)](2+) in Aqueous Solution. *Chem. - Eur. J.* **2010**, *16*, 5889−5894.
(97) Lawson Daku, L.; Hauser, A. Ab Initio Molecular Dynamics Study of an Aqueous Solution of [Fe (bpy) 3](Cl) 2 in the Low-Spin and in the High-Spin States. *J. Phys. Chem. Lett.* **2010**, *1*, 1830−1835.
(98) Haldrup, K.; et al. Guest-Host Interactions Investigated by Time-Resolved X-ray Spectroscopies and Scattering at MHz Rates: Solvation Dynamics and Photoinduced Spin Transition in Aqueous $Fe(bipy)_3^{2+}$. *J. Phys. Chem. A* **2012**, *116*, 9878−9887.
(99) Czerwieniec, R.; Yu, J.; Yersin, H. Blue-Light Emission of Cu(I) Complexes and Singlet Harvesting. *Inorg. Chem.* **2011**, *50*, 8293−8301.
(100) Kaeser, A.; et al. Heteroleptic Copper(I) Complexes Prepared from Phenanthroline and Bis-Phosphine Ligands. *Inorg. Chem.* **2013**, *52*, 12140−12151.
(101) Zhang, Q.; Zhou, Q.; Cheng, Y.; Wang, L.; Ma, D.; Jing, X.; Wang, F. Highly Efficient Green Phosphorescent Organic Light-Emitting Diodes Based on CuI Complexes. *Adv. Mater.* **2004**, *16*, 432−436.

DOI: 10.1021/acs.jpca.5b03842
J. Phys. Chem. A 2015, 119, 7026−7037